Comparison of Calculation Methods of Braided Shield Cable Transfer Impedance Using FSV Method

Jinjun Bai [1], Gang Zhang [1], Lixin Wang [1], Alistair Duffy [2], Chao Liu [1], and Tianyu Shao [1]

[1] School of Electrical Engineering and Automation
Harbin Institute of Technology, Harbin 150001, China
hitbaijinjun@163.com, zhang_hit@hit.edu.cn, wlx@hit.edu.cn, lcathit@163.com, shty.hit@gmail.com

[2] School of Engineering
De Montfort University, Leicester LE1 9BH, UK
apd@dmu.ac.uk

Abstract ─ This paper presents the results of recent work based on finite element numerical modeling in Ansoft HFSS to predict the surface transfer impedance of braided coaxial cables. Two approaches to the cable 3D modeling are investigated: (1) a simplified structural model, and (2) a rigorous structural model of braided shielded cable which is designed in Pro/Engineer software. The proposed approach provides a robust method that can overcome the challenges in the existing theoretical analysis. Factors influencing the cable transfer impedance are analyzed in detail. The validity of this simulation method is verified by comparison with a new measurement method based on time-domain response of two cable samples. The reliability of these two sets of data is analyzed by use of the feature selective validation method.

Index Terms ─ Braided shield cable, feature selective validation method, finite element method, transfer impedance.

I. INTRODUCTION

The structure of a cable shielded layer, especially for braided cables, is complex compared with other forms of shielding. These complexities can arise through design approaches such as the use of copper-clad-aluminum, non-copper braids, hybrid shields, where braided wires form part of a more complex shield, or where spindles are loaded with different diameter braid wires. Also, there are many rhombic apertures in the shielded layer, and the weaving of the braid makes the equivalent thickness of the shielded layer change. The basic modeling tools of existing EM simulation software cannot easily model complex braid structures because of the high level of complexity and fine detail required. Consequently, the calculation of the braided shield cable transfer impedance [1] which is an indicator of the quality of cable shield, relies on analytical methods in most cases.

Several theoretical models of the transfer impedance have been discussed in the literature. These include the models described by Tyni, Vance, Sali, Kley, Demoulin, etc. [2]-[6]. The predictions of these approaches are excellent at low frequencies (under 10 MHz), but become larger than the measurement results at high frequencies. This difference may be attributed to non-inclusion eddy currents caused by magnetic field between the two layers of the braid, which will produce unpredictable attenuation values for the transfer impedance [7]. So an improved model for the calculation of transfer impedance was proposed in [7] and provided better prediction results. However, the analytical method is, itself, empirical and therefore not suited without additional rigorous analysis to analyze novel structures, materials or non-uniform structures.

At present, common numerical analysis methods for solving the problem of field-line coupling are the MoM method, the FDTD method and the FEM method. Reference [8] used the MoM method to analyze the electromagnetic radiation effect of the aperture on a coaxial cable, providing a reference for the numerical computation of the

Submitted On: August 14, 2013
Accepted On: October 11, 2014

shielded cable transfer impedance. Reference [9] uses the Z transform and FDTD method for solving the radiation leakage of coaxial cable in free space. However, both methods have a common drawback: for the spindly structures, the diameter is relatively large compared with the size of the smallest elements, thus placing heavy computational demands making it difficult to get an accurate figure for the transfer impedance of shielded cable. Reference [10] first proposed using the finite element method to calculate the transfer impedance matrix of multi-core shielded cable. And more subtle FEM models of braided shield cable were discussed in [11].

This paper studies the braided shield cable structure, and then constructs two FEM models based on the work in [12]. In addition, factors influencing the cable transfer impedance are analyzed in detail using the proposed models. The performance of the proposed models is validated by use of the Feature Selective Validation (FSV) method [13] through comparing the simulated and measured results.

The FSV method is a kind of numerical calculation of the validation rating recommended in IEEE Standard 1597.1, which can give qualitative and quantitative results with regard to the agreement between data sets. The results of the FSV methods are given in different layers. In this paper, the single value and qualitative histogram results of the Global Difference Measure (GDM) results, GDMtot and GDMc are used to show the agreement between results given by different methods. More details of this method can be found in [13].

The transfer impedance definition and its calculation are briefly summarized in Section II along with mathematical modeling using FEM in Section III. Section IV describes the construction of simplified and rigorous models of braided shield cable. The results given by different methods are compared and discussed in Section V. Further, factors influencing the transfer impedance are analyzed in Section VI. Section VII gives a summary and some concluding remarks.

II. TRANSFER IMPEDANCE DEFINITION AND ITS CALCULATION

Transfer impedance is defined as:

$$Z_{\mathrm{T}} = \frac{1}{I_0}\frac{\partial V}{\partial z}\Big|_{I=0}, \tag{1}$$

where $\partial V/\partial z$ is the RMS voltage per unit length of the uniform transmission line created by the inner surface of the shielding layer and the cable core. I_0 is the induced current flowing through the outer surface of the shielded layer. I is the current flowing through the core wire.

Generally, the theoretical expression [7] for the transfer impedance is given by:

$$Z_{\mathrm{T}} = Z_{\mathrm{d}} + j\omega(M_{\mathrm{h}} \pm M_{\mathrm{b}}) + Z_{\mathrm{e}}, \tag{2}$$

where Z_{d} is diffusion impedance due to the diffusion of the current induced in the shield. It describes the linkage between the fields inside and those outside at low frequencies. Its value decreases as the frequency increases. M_{h} is hole inductance caused by the direct leakage of the magnetic field through the rhombic holes of the shield. M_{b} is the braid inductance caused by the magnetic flux linkage between the inner and outer braided layers. Z_{e} is the extra inductance indicating the influence of eddy current caused by electromagnetic field between the inner and outer braid layers. The detail of these parameters can be found in [7].

III. MATHEMATICAL MODELING

Broadly speaking, three-dimensional Maxwell equations are the governing equations of electromagnetic field problems. However, under normal circumstances, in order to facilitate the modeling and obtaining a solution, the two Maxwell curl equations are used to obtain the Vector Helmholtz equation as the key equation [14]:

$$\nabla\times(\frac{1}{\mu_r}\nabla\times\boldsymbol{E}) - k_0^2\varepsilon_r\boldsymbol{E} = 0, \tag{3}$$

where μ_{r} is the relative magnetic permeability, k_0 is the wave number of the free space, $\boldsymbol{E}(x,y,z)$ is the corresponding vector of time-harmonic field, $\boldsymbol{E}(x,y,z,t) = R\left\{\boldsymbol{E}(x,y,z)e^{j\omega t}\right\}$, ε_{r} is the relative dielectric constant.

The function of equation (3) can be derived from variation principle:

$$F(\boldsymbol{E}) = \iiint_{\Omega} \left\{ \frac{1}{\mu_r} (\nabla \times \boldsymbol{E})(\nabla \times \boldsymbol{E}) - k_0^2 \varepsilon_r \boldsymbol{E}\boldsymbol{E} \right\} d\Omega = 0. \quad (4)$$

The boundary condition of the configuration illustrated in Fig. 1 shows the braided cable simulation model diagram, from outside to inside consisting of air, braided layer, the inner insulating layer, and the core wire. On the radiation surface, the boundary condition is:

$$(\nabla \times \boldsymbol{E})_{\tan} = jk_0 \boldsymbol{E}_{tan} - \frac{j}{k_0} \nabla_{\tan} \times (\nabla_{\tan} \times \boldsymbol{E}_{tan}) + \frac{j}{k_0} \nabla_{\tan} (\nabla_{\tan} \boldsymbol{E}_{tan}), \quad (5)$$

where $\boldsymbol{E}_{tan}$ is the tangential component of the surface electric field.

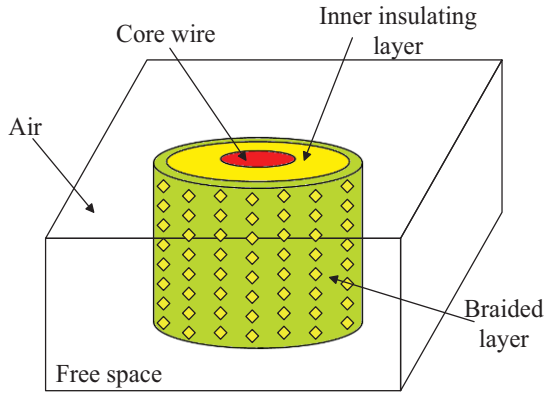

Fig. 1. Diagram of braided cable simulation model.

The two terminal cross sections of the shielded cable were set to PEC (Perfect Electrical Conductor, or Perfect E Condition) to stop the fields entering the cable through the ends. PEC can be described as:

$$\nabla(\varepsilon \boldsymbol{E}) = 0, \quad \hat{n} \times \boldsymbol{E} = 0. \quad (6)$$

A plane wave was chosen to be the excitation source. The plane wave can be described as:

$$E_{\text{inc}} = E_0 e^{-jk_0(\boldsymbol{kr})}, \quad (7)$$

where E_{inc} is the incident wave, E_0 is electric polarization vector, k_0 is wave number of free space, $\boldsymbol{k}$ is unit propagation vector, $\boldsymbol{r}$ is a position vector, $\boldsymbol{r} = x\hat{\boldsymbol{x}} + y\hat{\boldsymbol{y}} + z\hat{\boldsymbol{z}}$.

After $\boldsymbol{E}(x, y, z)$ is obtained, formula (1) can be redefined as:

$$\frac{\partial V}{\partial z} = \frac{1}{A_e} \iint_{S_e} \boldsymbol{E}_z d\boldsymbol{S}_e, \quad (8)$$

$$I_0 = \iint_{S_i} \sigma \boldsymbol{E} d\boldsymbol{S}_i, \quad (9)$$

where E_z is the longitudinal electric field component. $\boldsymbol{S}_e$ is the inner surface of the cable shield, $\boldsymbol{S}_i$ is its transversal surface as shown in Fig. 2. A_e is the area of $\boldsymbol{S}_e$. σ is the electrical conductivity of shield.

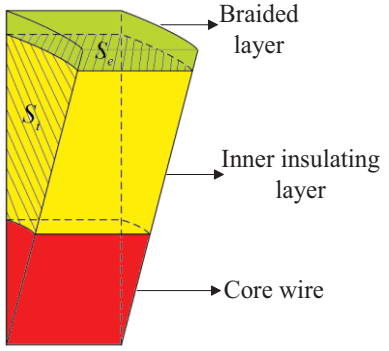

Fig. 2. Integral surfaces.

IV. MODEL DESCRIPTION

A. The simplified structural model

In order to decrease the complexity of the model and increase the simulation speed, the change of the equivalent thickness of the shielded layer caused by the braiding has been ignored in order to focus on the numerous rhombic holes on the shielded layer. Figure 3 shows the basic unit of braided shield. The key to create a simplified numerical structural model is to determine the side length of every rhombic hole, l_{rh}, and the horizontal and vertical distance of two adjacent holes, l_1, l_2, according to the known data of the cable. Figure 4 shows the simplified structural model. Once we know the structure parameter of the shielded layer, the parameters l_{rh}, l_1, l_2, can be described as in (10) to (13):

$$l_{rh} = \frac{W - Nd}{\sin(2\alpha)}, \quad (10)$$

$$l_1 = \frac{2\pi D_m}{C}, \quad (11)$$

$$l_2 = \frac{l_1}{\tan\alpha}, \tag{12}$$

$$W = \frac{2\pi D_m}{C}\cos\alpha, \tag{13}$$

where N is number of woven wires in a bundle. d is the diameter of the braided wire. C is the number of beams of the braid knitting. α is braiding angle. D_m is the diameter of the shield.

As the braiding effect is ignored, the effective thickness of shielded layer becomes a constant, so the thickness of shielded layer $T=2d$ when we use the simplified structure model:

$$D_m = D_0 + 4d, \tag{14}$$

where D_0 is the diameter of the insulating materials (inner diameter of shield).

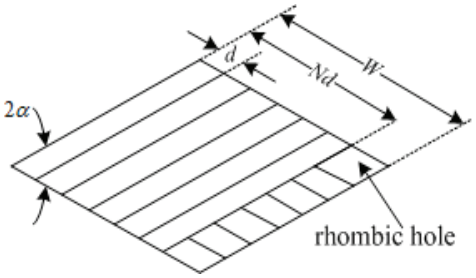

Fig. 3. Basic unit of braided layer.

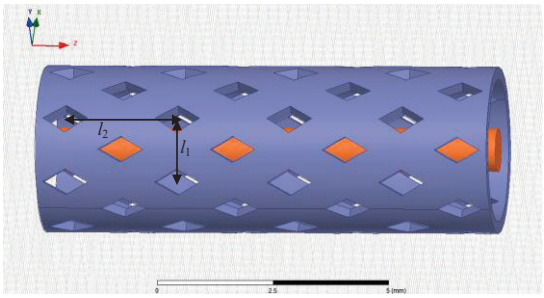

Fig. 4. The simplified structure model.

B. The rigorous structural model

Conversely, the rigorous structure model considered the change of the equivalent thickness of the shielded layer caused by braiding in and out of the weaving beams, as shown in Fig. 5. The cylindrical tube represents the shielded layer. The groove running on the tube represents the area that the weaving beam is not overlapping. The thickness is T=1.5*d*. The length of the long diagonal of the rhombic holes:

$$l_d = \frac{W - Nd}{\sin\alpha}. \tag{15}$$

The width of each knitting beam:

$$l_b = Nd. \tag{16}$$

The rest of the area of the tube represents the weaving beam overlapping, where the thickness of shielded layer T=2.5*d*.

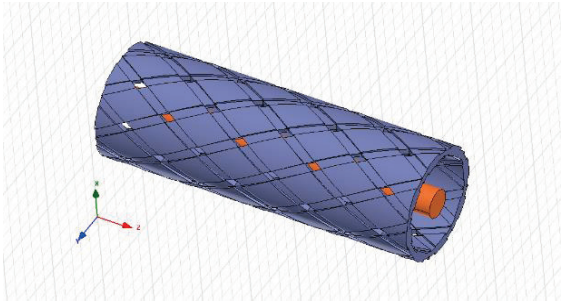

Fig. 5. The rigorous structure model.

V. RESULTS AND THE ANALYSIS OF FSV

In order to verify the aforementioned analytical or numerical methods, the models of TV cables SYV50-3 and SYV75-2-1 are established. Transfer impedance measurements of these two cables are performed using the method mentioned in reference [15]. The theoretical result is calculated according to formula (2) which comes from [7]. The simplified structure model and the rigorous structure model are shown in Figs. 4 and 5, respectively. Both of the models are calculated using the Ansoft HFSS software.

Parameters of SYV50-3 and SYV75-2-1 are shown in Table 1. D is the diameter of the core wire, D_0 is the diameter of the insulating materials (inner diameter of shield), C is the number of beams of the braid knitting, d is the diameter of the braided wire, N is number of woven wires in a bundle, p is the woven pitch, ε_r is the relative magnetic permeability, σ is electrical conductivity. Both the cable's core wire material is copper, the insulating layer is solid polyethylene, and the shielded layer material is copper.

For a more intuitive comparison, the results of measurement, theoretical calculation and simulation results of SYV50-3 and SYV75-2-1 are shown in Figs. 6 and 7, respectively. It can be seen from the figures that both the analytical and numerical methods can give generally reasonable

results, and the difference between them and measurement results is difficult to be identified by visual assessment. So the FSV method is introduced to compare the simulated or analytical results with measurement result to show the advantage or disadvantage of these methods. In addition to the quantitative assessment of data agreement, the FSV method can give the qualitative assessment described by natural language which cannot be shown by root-mean-square error or residual.

Table 1: Parameters of SYV50-3 and SYV75-2-1

Parameters	SYV50-3	SYV75-2
D (mm)	0.9	0.4
D_0 (mm)	2.95	2.3
C	16	16
d (mm)	0.12	0.11
N	6	6
p (mm)	18.8	23
ε_r	2.029	2.25
σ (S/m)	5.8e^7	5.8e^7

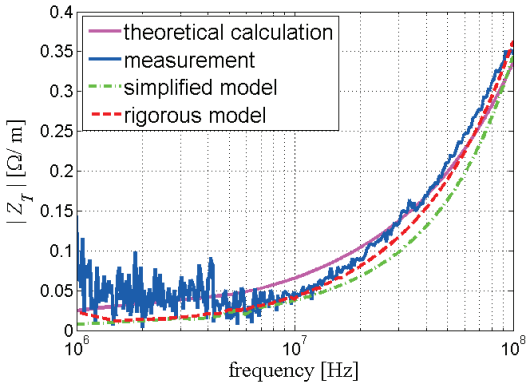

Fig. 6. Results for SYV50-3.

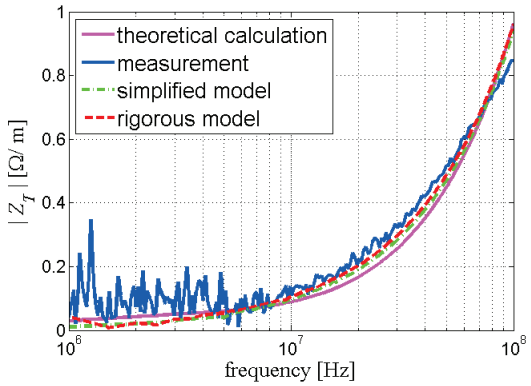

Fig. 7. Results for SYV75-2-1.

Figures 8 and 9 outline the GDMc results. Specifically, GDMc results can mirror the distribution of survey results given by a group of experts who are asked to describe the agreement between data sets using natural language (Excellent, Very Good, Good, etc.). Table 2 shows the GDMtot results which are the quantitative measure of global difference between predicted results and measurement result. The smaller GDMtot value the better accuracy of method.

It is demonstrated by the FSV results that the FEM models can give more accurate predictions than the analytical method for both of the cables. And the results of the rigorous structure are more accurate than the simplified one for the SYV50-3. But for the SYV75-2-1, there is no obvious difference between the two FEM models. Generally, the simplified structure model is a good compromise between the modeling complexity and accuracy as indicated in Table 2. It should be noted that even the analytical result can show "Good" agreement with measurement results.

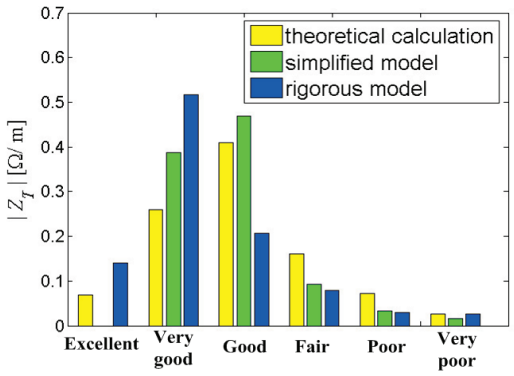

Fig. 8. Comparison of GDMc results for SYV50-3.

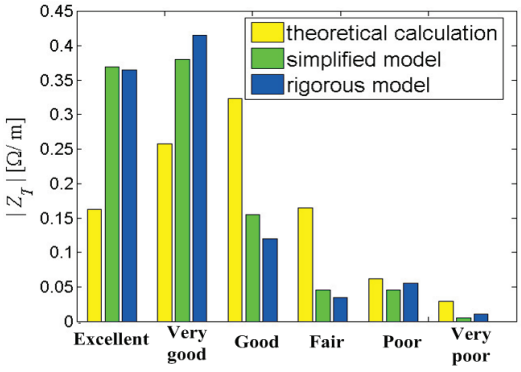

Fig. 9. Comparison of GDMc results for SYV75-2-1.

Table 2: GMDtot results of the three models

GDMtot	Theoretical Calculation	Simplified Model	Rigorous Model
SYV50-3	0.40	0.31	0.28
SYV75-2-1	0.37	0.20	0.21

VI. INFLUENCING FACTORS OF TRANSFER IMPEDANCE

In order to analyze the influencing factors of braided shielded cable transfer impedance, four important parameters including simulation length of the cable, shielding material, inner diameter of the shield and diameter of the braided wire are discussed.

A. Simulation length of cable

Theoretically, the simulation length of the cable has no effect on the simulation results. We chose the former mentioned rigorous structure model of cable SYV50-3 as an example. Different lengths (10 mm, 15 mm and 20 mm) were simulated. Figure 10 (a) shows the results. These results are consistent in the whole frequency range, noting the observation made later in this section. This indicates that the length of the cable in the simulation does not affect the simulation results when the cable is electrically short. However, the computer performance limits the length of the cable which can be simulated in a reasonable period of time. The simulation times of these three models are 10 hours, 12.5 hours and 38 hours respectively. It has the exponential growth trend. The CPU is Pentium (R) Dual-Core E5300 @ 2.6 GHz with 2 GB memory. The program was set parallelized.

B. Shielding material

In this section, the influence of shielding layer materials is analyzed. We chose the former mentioned rigorous structure model of cable SYV75-2-1 as an example. Three different materials: copper, tin and steel were simulated. As shown in Fig. 10 (b), at low frequency, the shielding effectiveness of copper is better than the other two materials. As the frequency went up to 30 MHz, the copper shielding becomes worse. So when the cable is used in low frequency range (less than 30 MHz), cables with copper shielding are recommended, and when the cable is used in the higher frequency range (more than 30 MHz), tin or steel may make more efficient shields for this geometry.

C. Inner diameter of the shield

The influence of inner diameter of shield (D_0 mentioned in Table 1) on the transfer impedance is observed based on the rigorous structure model of cable SYV50-3. The impedance for different D_0 (2.91 mm, 2.93 mm, 2.95 mm, 2.97 mm and 2.99 mm) are shown in Fig. 10 (c). It can be seen that the increase of D_0 leads to the reduction of the transfer impedance. For this reason, the shielding effectiveness will improve, but the cost will increase.

D. Diameter of the braided wire

In this section, the former mentioned rigorous structure model of cable SYV50-3 is also used to analyze the influence of braided wire diameter (d mentioned in Table 1). Figure 10 (d) shows the change of the transfer impedance for different d (0.115 mm, 0.118 mm, 0.12 mm, 0.122 mm and 0.125 mm). It is shown that with the increase of d, the transfer impedance may decrease. As a result, the shielding effectiveness can be improved. Accordingly, the costs of cable production will increase.

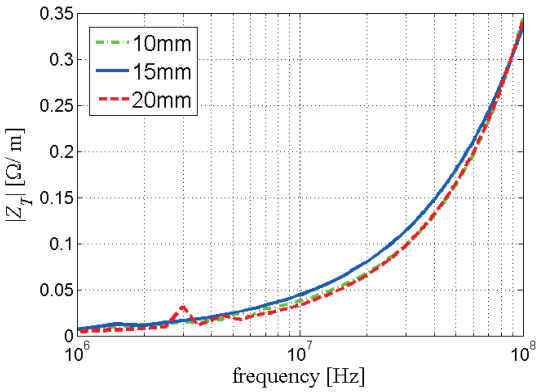

(a) Simulation length

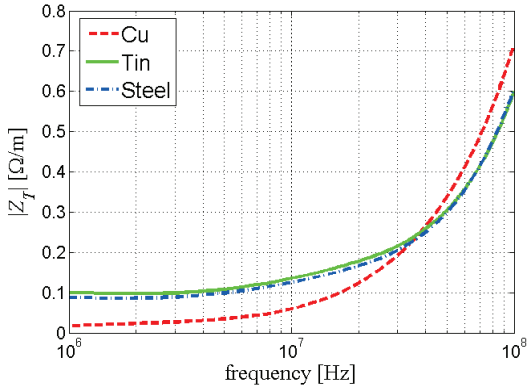

(b) Shielding material

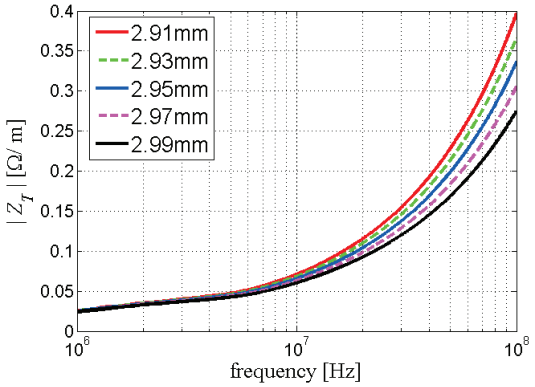

(c) Diameter of the insulating materials

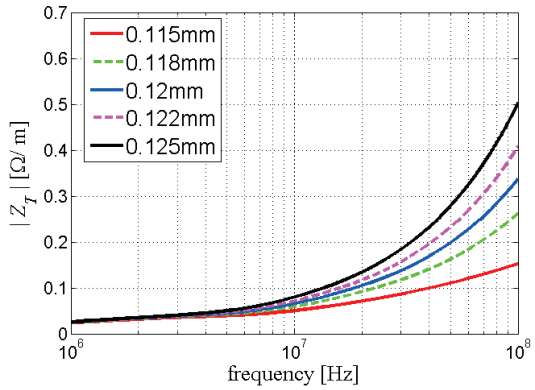

(d) Diameter of the braided wire

Fig. 10. Influence of different parameters.

VII. CONCLUSION

Several methods for transfer impedance calculation of braided shielded cable have been discussed. Two 3D models: the simplified structure model and the rigorous structure model have been modeled using Ansoft HFSS. The results of both models are verified by measurement results and compared with theoretical calculation using the FSV method. From the FSV analysis, we can see that the simplified structure model provides a reasonable approximation to the measurement results. The results of the rigorous structure are more accurate than the simplified one; however, one goal of analyses such as these is to investigate the question "how efficient can the simulation be made?" This paper has suggested that a reasonable level of simplification can lead to reasonable computational demands with only a small reduction in the accuracy of the results obtained.

Finally, factors influencing the transfer impedance, including simulation length of cable, material of the shielding layer, inner diameter of the shield and diameter of the braided wire, were investigated as examples of the application of the approach proposed in this paper.

REFERENCES

[1] S. A. Schelkunoff, "The electromagnetic theory of coaxial transmission lines and cylindrical shields," *Bell Syst. Tech. J.*, vol. 13, no. 4, pp. 532-579, 1934.

[2] M. Tyni, "The transfer impedance of coaxial cables with braided outer conductor," *Digest of the 10th International Wroclaw Symposium on EMC*, pp. 410-419, 1976.

[3] E. F. Vance, "Shielding effectiveness of braided-wire shields," *IEEE Trans. Electromagnetic Compatibility*, vol. EMC-17, no. 2, pp. 71-77, 1975.

[4] S. Sali, "An improved model for the transfer impedance calculations of braided coaxial cables," *IEEE Trans. Electromagnetic Compatibility*, vol. 33, no. 2, pp. 139-143, 1991.

[5] T. Kley, "Optimized single-braided cable shields," *IEEE Trans. Electromagnetic Compatibility*, vol. 35, no.1, pp. 1-9, 1993.

[6] B. Demoulin and P. Degauque, "Shielding effectiveness of braids with high optical coverage," *Proceedings of the International Symposium on EMC*, Zurich, pp. 491-495, 1981.

[7] W. Xiaoling, et al., "An improved model for the transfer impedance calculations of braided coaxial cables," *IEEE 7th International Power Electronics and Motion Control Conference (IPEMC)*, vol. 2, 2012.

[8] T. Liu and L. Zhang, "Electromagnetic radiation effect of the aperture on a coaxial cable," *Electronic Components & Device Applications*, vol. 12, no. 5, pp. 90-94, 2010.

[9] F. Linlin, "Leakage radiation analysis of coaxial cable based on FDTD," *Harbin Engineering University*, Harbin, 2010.

[10] M. Feliziani and F. Maradei, "A FEM approach to calculate the impedances of shielded multiconductor cables," *IEEE Trans. Magnetics*, vol. 2, no. 2, pp. 1020-1025, 2002.

[11] R. Otin, J. Verpoorte, and H. Schippers, "Finite element model for the computation of the transfer impedance of cable shields," *IEEE Trans. Electromagnetic Compatibility*, vol. 53, no. 4, pp. 950-958, 2011.

[12] C. Liu, A. Duffy, and L. Wang, "Calculation of braided shielded cable transfer impedance based on FEM method," *The 29th International Review of Progress in Applied Computational Electromagnetics*, Monterey, CA, 2013.

[13] "IEEE standard for validation of computational electromagnetics computer modeling and simulations," *IEEE STD 1597.1-2008*, pp. 1-41,

2008.
[14] J. Jin, "The finite element method in electromagnetics," 2nd ed., *Hoboken, NJ: Wiley*, 2002.
[15] B. Vanlandschoot and L. Martens, "New method for measuring transfer impedance and transfer admittance of shields using a triaxial cell," *IEEE Trans. Electromagnetic Compatibility*, vol. 39, no. 2, pp. 180-185, 1997.

Jinjun Bai was born in Jilin, China, on January 21, 1991. He received the B.Eng. degree in Electrical Engineering and Automation from the Harbin Institute of Technology, Harbin, China, in 2013. He is currently working towards the Ph.D. degree in Electrical Engineering at the Harbin Institute of Technology, Harbin, China. His research interests include computational electromagnetics and electromagnetic compatibility of indoor power line communication systems.

Gang Zhang received the B.Sc. in Electrical Engineering from China University of Petroleum, Dongying, China, in 2007, and the M.Sc. and Ph.D. degrees in Electrical Engineering from Harbin Institute of Technology (HIT), Harbin, China, in 2009 and 2014, respectively.

He is now with the Faults Online Monitoring and Diagnosis Laboratory at Harbin Institute of Technology. His research interests include analysis of electromagnetic compatibility, electromagnetic simulation, and the validation of CEM.

Lixin Wang received the B.S. degree in Electrical Engineering from Nankai University, Tianjin, China, in 1988, and the M.S. and D.Sc. degrees in Electrical Engineering from Harbin Institute of Technology (HIT), Harbin, China, in 1991 and 1999, respectively.

He is currently a Professor of Power Electronic and Electric Drives at HIT. He conducts research with Faults Online Monitoring and Diagnosis Laboratory, HIT, on a wide variety of topics including electromagnetic compatibility at the electronic system level, aircraft electromechanical fault diagnosis expert system and Prediction and Health Management (PHM) of Li-ion battery.

Alistair Duffy was born in Ripon, U.K., in 1966. He received the B.Eng. (Hons.) degree in Electrical and Electronic Engineering and the M.Eng. degree from the University College, Cardiff, U.K., in 1988 and 1989, respectively. He received the Ph.D. degree from Nottingham University, Nottingham, U.K., in 1993 for his work on experimental validation of numerical modeling and the MBA from the Open University in 2003.

He is currently a Reader in electromagnetics at De Montfort University, Leicester, U.K. He is the author of over 150 articles published in journals and presented at international symposia. His research interests include CEM validation, communications cabling, and technology management.

Duffy is a Fellow of the Institution of Engineering and Technology (IET) and a Member of the International Compumag Society and the Applied Computational Electromagnetics Society. He is a Member of the IEEE EMC Society Board of Directors and is the Chair of the IEEE EMC Society Standards Development and Education Committee.

Chao Liu received the B.Sc. and M.Sc. degrees in Electrical Engineering from Harbin Institute of Technology (HIT), Harbin, China, in 2005 and 2007, respectively. He is currently working towards the Ph.D. degree at HIT and involved in the research of electromagnetic compatibility of test system and electromagnetic simulation of cables.

Tianyu Shao received the B.Sc. in Electrical Engineering from Harbin Institute of Technology (HIT), Harbin, China, in 2012. He is currently working towards the M.Sc. degree at HIT and involved in the research of electromagnetic compatibility of indoor power line communication systems.